

Oleic Acid-Influenced Graphene Oxide from Sugarcane Bagasse as Waterproofing Admixture in Rendering Mortar (external wall finishing)

Jewel Angelique D. Panadero* and Haziell Marie P. Baybayon
Physics Department
Central Mindanao University
University Town, Musuan, Maramag, Bukidnon, 8714 Philippines
*panaderojewel@gmail.com

Date received: October 11, 2022
Revision accepted: March 5, 2025

Abstract

This study prepared a hydrophobic rendering mortar using oleic acid-influenced graphene oxide (OA-GO) as an admixture. The graphene oxide (GO) used in this study was synthesized from sugarcane bagasse. Oleic Acid (OA) was used as an influencing agent of GO in making the OA-GO admixture. Rendering mortars with GO and OA admixtures were fabricated to differentiate the OA-GO admixture's effects. FT-IR, SEM, and XRD were performed to confirm the synthesized GO from sugarcane bagasse. Hydrophobicity was evaluated through a contact angle test, with subsequent statistical analyses revealing significant disparities among the tested mortars and across varying time intervals. Results showed that the use of OA-GO admixture corresponds to a higher contact angle of $98.50^\circ \pm 3.68^\circ$ and $115.82^\circ \pm 10.86^\circ$ after curing for 7 and 28 days, respectively. Thereby confirming its hydrophobicity among other tested mortars. Also, the compressive strength test results showed an increased compressive strength of the mortar with OA-GO admixture by almost twice, 1.82, that of the mortar with OA alone. It is concluded that the GO used in producing the OA-GO admixture equalizes the downside effect of OA. The results helped understand the effectiveness of sugarcane bagasse as a primary material in making an admixture to create a hydrophobic rendering mortar for external wall finishing.

Keywords: admixture, graphene oxide, oleic acid, sugarcane bagasse, waterproofing

1. Introduction

Concrete degradation is usually due to water ingress from uncontrolled environmental factors such as rain and hot weather. To mitigate this problem, it is good to consider appropriate measures that will help prevent water ingress

on a concrete material such as an external wall (Luan *et al.*, 2014; Muzenski *et al.*, 2014). In this case, hydrophobic rendering mortar is necessary for external wall finishing. Adding a waterproofing admixture to a rendering mortar composition is one of the methods of making concrete waterproof. The use of expensive and locally inaccessible equipment in producing hydrophobic rendering mortar is also a factor. For instance, a study using a commercialized hydrophobic agent (silicone) as a waterproofing additive in mortars reported that adding a hydrophobizing agent in mortars decreased water absorption and increased water contact angle, thus making the modified mortar hydrophobic. However, the compressive strength of the modified mortars with hydrophobizing agents was decreased compared to the blank ones (no admixture) (Luan *et al.*, 2014). Another study using a hydrophobizing agent in rendering mortars utilized six types of waterproofing additives to evaluate their capillary water absorption. The study showed that powdered silicone and sodium oleate (unsaturated fatty acid) are the most effective additives in rendering mortars to repel water (Lanzón and García-Ruiz, 2009). However, characterization was not conducted to test the compressibility of the rendering mortars with waterproofing additives.

The use of additives and admixtures in modifying a rendering mortar into hydrophobic is a practical step in protecting a concrete material. One of the most accessible waterproofing agents is oleic acid. Oleic acid (OA) is an unsaturated fatty acid that a hydrophobic admixture usually has. Naval Civil Engineering Laboratory (2009) reported the use of OA as a waterproofing agent in concrete. However, the addition of OA to Portland cement showed a decrease in compressive strength with its increasing increments. Other effects reported were reduced water requirement of normal consistency, extended setting time, and improved rheological properties of cement-based materials (Ma *et al.*, 2013).

On the other hand, Graphene oxide (GO) is known to have the capability to increase the compressive strength of a material. An OA may contain a waterproofing capability but does not guarantee a strong hold of concrete composition. Therefore, influencing the GO with OA may be a possibility to equalize its negative side effect on the concrete matrix. Since using OA alone as a waterproofing agent will decrease the compressive strength of the mortar, using GO as an admixture powder may help equalize the downside effect brought by OA. GO has unique features such as its rough surface and a functional group that favors the mechanical behavior of cement. Reinforcing GO is beneficial in terms of its superior aspect ratio compared to conventional fibers (Chuah *et al.*, 2014). Furthermore, GO appears to be an ideal candidate to enhance the properties of a cement-based composite among nanofillers such as carbon nanotubes and nano silica. In addition to the advantages of using GO, its intrinsic properties strengthen the brittle cement matrix, similar to

carbon nanotubes (Chuah *et al.*, 2014). Previous research also used commercialized or high-value materials to obtain concrete impregnated with GO powders in order to prove its effectiveness and durability (Somanathan *et al.*, 2015). Although, the aforementioned studies have stated that GO is an appealing candidate for increasing the compressive strength of a concrete, there were no studies conducted or suggesting the use of synthesized GO from agrowaste as hydrophobic admixture in external wall finishing mortar.

In this study, a novel approach is introduced whereby graphene oxide (GO) serves as a reinforcing agent alongside oleic acid (OA) to produce a hydrophobic admixture for rendering mortar. In contrast to conventional methods that depend solely on commercialized and readily available hydrophobic admixtures, this research integrates GO and OA to improve both waterproofing and compressive strength. Additionally, GO synthesized from sugarcane bagasse is employed, presenting a sustainable solution. This innovative strategy shows potential for developing durable and high-performance hydrophobic mortar mixtures.

2. Methodology

2.1 Preparation of graphene oxide and oleic acid-influenced graphene oxide

The agro-waste sugarcane bagasse was acquired from the Sugarcane Milling Company, Maramag, Bukidnon, Philippines. Oleic acid (5-30 % at 0.375 mL) purchased at Elmar Marketing, Iligan City, Philippines. Industrial-grade ferrocene ($C_{10}H_{10}Fe$), purchased at Theo-Pam Trading Corporation, Pasay City, Philippines, was used in the study as a metal catalyst in the oxidation process of the bagasse.

The method of synthesizing graphene oxide (GO) was adapted from the study of Somanathan *et al.* (2015) with slight modifications. The juice was eliminated from the sugarcane bagasse, and the remaining fiber was taken (Figure 1a). The obtained fiber was crushed and ground well. This process was repeated several times to obtain 0.5 g of fine powder. A crucible was used as container with 0.1 g of ferrocene and the fine powder and was put directly into a muffle furnace at 300°C for 10 minutes. The synthesized powder was then washed using acetone and air dried to obtain a fine powder that is subjected for further analysis. For influencing the oleic acid to the produced GO, the synthesized GO (0.5 g) was added to the 5 mL oleic acid and allowed the reaction to perform for 1 hr at 50 °C under stirring.

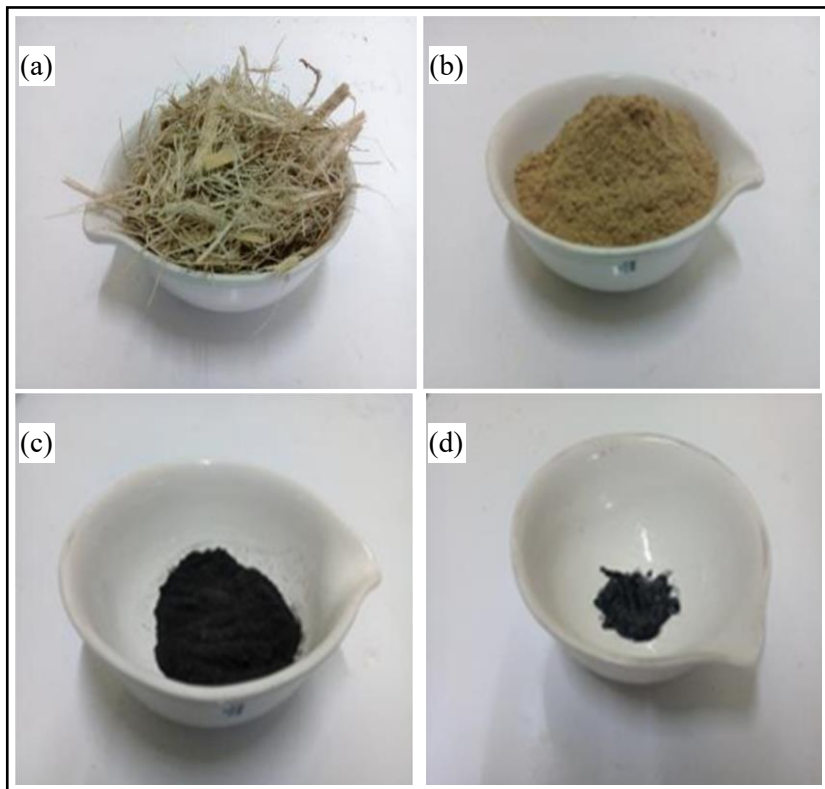


Figure 1. Images of the overall preparation of the oleic acid-influenced GO: sugarcane bagasse (a), powdered bagasse (b), graphene oxide (c), oleic acid-influenced GO (d)

2.2 Testing procedures of GO and OA-GO

The confirmation of the functional groups present in the synthesized graphene oxide was performed by Fourier Transform Infrared (FT-IR) Spectroscopy Analysis (IRAffinity-1S, Shimadzu, Japan). The sample was also subjected to a full scan X-Ray Diffraction (XRD) analysis (Maxima-7000, Shimadzu, Japan) set at 3.0 to 90°, 2 θ / θ angle generated from Cu- α radiation source ($\lambda=1.54\text{\AA}$). Moreover, the structural characteristics and morphology of graphene oxide was examined using Scanning Electron Microscope (SEM) (5300, JEOL, Japan).

Due to its paste-like texture, the OA-GO's efficacy as waterproofing admixture was tested using two methods: the water dispersion test, and as

admixture in rendering mortar mix and testing it through contact angle test. For the water dispersion test, this study compares the collected GO and OA-GO by immersing them in water to assess their stability in polar solvents.

2.3 Fabrication of hydrophobic mortar

The materials used for mixing and preparing mortar were thermostated at room temperature ranging from 20 - 30°C. The molds used for rendering mortar are made of steel and are nonreactive with concrete containing Portland or other hydraulic cement per the ASTM C192M-15 (2015) standards. The mortars prepared were reference mortar 0.00% (M1), mortar with 0.05% GO (M2), mortar with 0.05% OA-GO (M3), and mortar with 0.05% OA (M4).

The 0.05% OA-GO admixture was first mixed with the sieved sand until its homogeneity was attained. It was thoroughly mixed without the addition of water to ensure the evenness of the composite. The sand with the admixture was then allowed to blend for 24 hours. The water was added in increments until the mortar composite appeared homogenous. The cement-sand ratio is 1:3, while the water to cement ratio (w/c) was 0.4 (Bediako *et al.*, 2012).

Following the ASTM C192M-15 (2015) standards for curing, the molds were covered immediately with a non-absorptive, nonreactive plate or tough sheet to prevent the evaporation of water. This experiment used aluminum foil as the sheet to cover the specimen to prevent moisture loss. Approximately 48 hours after casting, the specimens were removed from the molds. The specimens were then cured at $23.0 \pm 2.0^\circ\text{C}$ from the casting of the specimen until the moment of the test.

2.4 Testing Procedures

Reference mortar, mortar with 0.05% GO, mortar with 0.05% OA-GO, and mortar with 0.05% OA with sizes of 50 x 50 x 50 mm, were prepared and brought out for 7 and 28 curing days for the compressive strength test following the ASTM C 109 (2002) using the Universal Testing Machine (WE-C1000D). Another set of specimens with the exact dimensions was also prepared for the contact angle analysis (Luan *et al.*, 2014).

2.5 Statistical analysis

Statistical comparisons were conducted using various tests to elucidate differences in contact angle measurements among the experimental groups (M1, M2, M3, and M4) and over time (7th and 28th day).

2.5.1 One-Way Analysis of Variance (ANOVA)

One-way ANOVA tests were performed on the 7th and 28th day to assess the differences in contact angle measurements among the experimental groups (M1, M2, M3, and M4). The significance of variations in contact angle values was determined based on the F-statistic and associated p-values.

2.5.2 Post Hoc Analysis

Following significant findings from the one-way ANOVA tests, post hoc analysis was carried out to identify specific differences between individual groups. This analysis facilitated a deeper understanding of the differences in contact angle measurements among the mortars: reference mortar 0.00% (M1), mortar with 0.05% GO (M2), mortar with 0.05% OA-GO (M3), and mortar with 0.05% OA (M4).

2.5.3 Paired t-Tests

Paired t-tests were conducted to investigate changes in contact angle measurements within each experimental group between day 7 and day 28. The results of these tests provided insights into the temporal evolution of surface properties, highlighting any significant alterations in contact angle over the designated time periods.

2.5.4 One-Sample t-Tests

Additionally, one-sample t-tests were utilized to determine whether the measured contact angle values deviated from the standard value of 90°, indicating hydrophobic or hydrophilic properties. This analysis enabled the classification of contact angles as either hydrophobic (> 90°) or hydrophilic (< 90°) within each experimental group and time point.

3. Results and Discussion

3.1 Graphene oxide Characterization

The XRD results, shown in Figure 2, illustrates two peaks determined to be at $2\theta = 23.15^\circ$ and $2\theta = 13.12^\circ$. The peak found at $2\theta = 23.15^\circ$ is between that of the graphene oxide and the graphitic phase (Jeong *et al.*, 2009). This intermediate peak may be attributed to the unoxidized graphene domains during the oxidation process. Moreover, the formation of a new peak at $2\theta = 13.12^\circ$ with an interlayer distance of 0.77 nm is closely related with the findings of Krishnamoorthy *et al.* (2013), where the peak's shift indicated the transition from the graphitic to the oxidized phase.

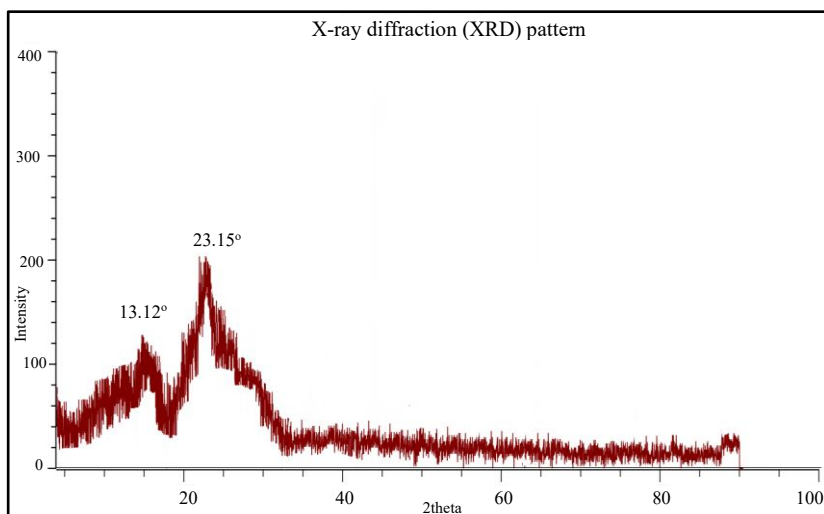


Figure 2. X-Ray Diffraction pattern of graphene oxide

The FT-IR spectroscopy results of the graphene oxide is shown in Figure 3. The characteristic peaks were observed at 3393.49 cm^{-1} , 1700.70 cm^{-1} , and 861 cm^{-1} . The peak at 3393.49 cm^{-1} corresponds to the strong and broad absorption of hydroxyl (-OH) groups bonded to the carbon backbone (Romani, 2015; Song *et al.*, 2014). The peak at 1700.70 cm^{-1} represents the stretching vibration modes and adsorption bands of C=O in carboxylic acid and carbonyl groups (Somanathan *et al.*, 2015; Song *et al.*, 2014). Meanwhile, the peak at 861 cm^{-1} is attributed to the stretching of C-O-C and C-O, which are associated with oxygen functionalities bonded to the carbon backbone (Romani, 2015).

The presence of oxygen-containing functional group, C=O, confirms the successful oxidation of graphite into GO, aligning with previous studies (Song *et al.*, 2014; Zhou *et al.*, 2011; Zhang and Pan, 2011; Shen *et al.*, 2011). Additionally, the detection of C=C groups indicates that although oxidation occurred, the layered graphite structure remained intact, consistent with the findings of Song *et al.* (2014).

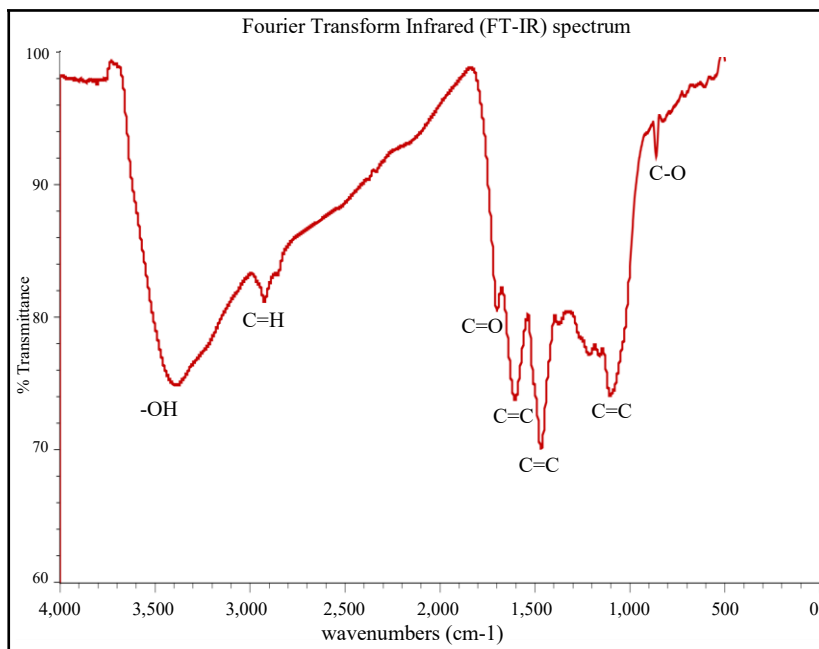


Figure 3. FT-IR spectra of graphene oxide

The morphological structure of the sample was confirmed by SEM. Results showed that the lamellar structure of the sample as well as the wrinkled surface of the sheet (Figure 4a) is in good agreement with the reported studies (Alam *et al.*, 2017; Krishnamoorthy *et al.*, 2013). Thicker edges were also noticed in the micrographs. This is due to the oxygen-containing functional groups that were usually found at the edges of GO films.

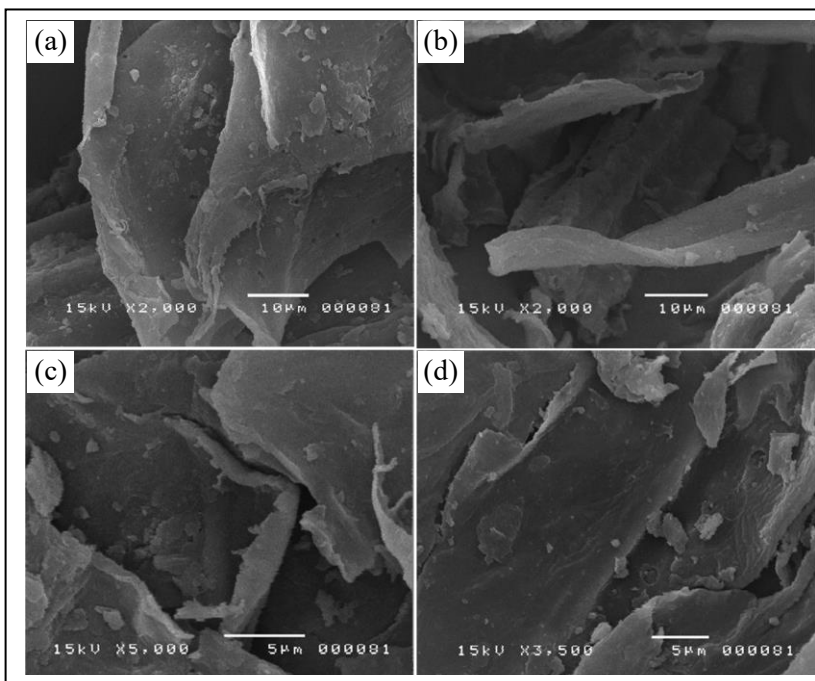


Figure 4. SEM micrographs of graphene oxide

3.2 Water dispersion test

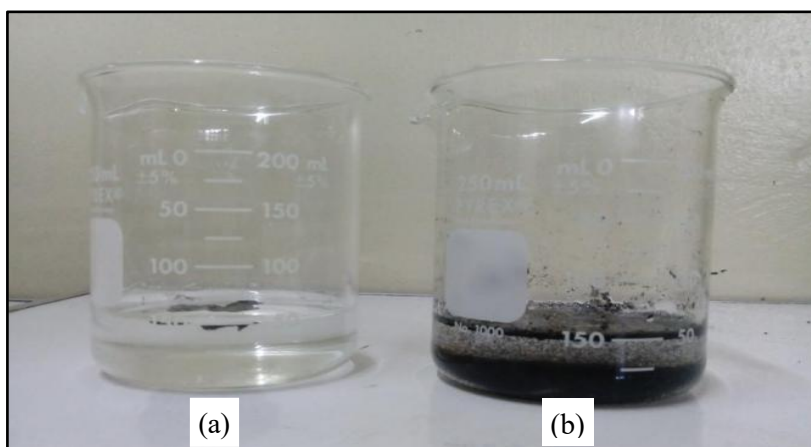


Figure 5. Water Dispersion Test: OA-GO (a), GO (b)

The dispersion test determined the stability of GO and OA-GO in polar solvent. The experiment used water as the polar solvent. GO remained permanently suspended in water, whereas OA-GO easily floated in the polar solvent (Figure 5). This finding indicates that GO has polar characteristic and is hydrophilic, while OA-GO exhibits hydrophobic nature due to the presence of oleic acid.

3.3 Contact angle measurement

The contact angle tests compared contact angles among different experimental groups on the 7th and 28th day. Statistical analyses, including one-way ANOVA, paired t-tests, and one-sample t-tests, examined changes over time and assessed the hydrophobicity of the measured contact angles.

Table 1 presents the statistical comparisons conducted using ANOVA tests. The results revealed a significant difference in contact angles among the treatment groups on both the 7th day ($F = 31.38, p < 0.0001$) and the 28th day ($F = 55.66, p < 0.0001$). This confirms that the type of admixture used, particularly the OA-GO combination, had a measurable impact on the hydrophobicity of the mortar. The low p-values (< 0.0001) indicate that these differences are highly significant and not due to random variation. Since the trend remained consistent over time, the effect of the admixtures appears to be stable.

Post hoc analysis clarified these differences by grouping the treatment conditions into statistically distinct subsets. M1 (0.00% admixture) and M2 (0.05% GO) fell within the same Tukey subset, indicating that their contact angles were not significantly different. This suggests that adding GO alone does not substantially alter water interaction compared to plain mortar, likely due to GO's hydrophilic nature (Rezaee *et al.*, 2015; Junaidi *et al.*, 2018). In contrast, M3 (0.05% OA-GO) had the highest contact angle and formed its own subset, confirming that the combination of OA and GO significantly enhances hydrophobicity. This improvement is likely due to OA modifying the behavior of GO, reducing its hydrophilicity and allowing it to function as a hydrophobic agent in mortar. Studies have shown that to consider concrete as hydrophobic, its water contact angle must exceed 90° (Barnat-Hunek and Smarzewski, 2015; Sharma and Sharma, 2021; Di Mundo *et al.*, 2018). This study confirmed its ability to enhance water repellency over time, as the OA-GO admixture resulted in mean contact angles of 98.50 ± 3.68 on the 7th day and 115.82 ± 10.86 on the 28th day,.

Meanwhile, M4 (0.05% OA) had the lowest contact angle and was placed in a separate subset, highlighting its significant difference from all other groups. This suggests that OA alone increases water absorption, possibly by altering cement hydration and increasing porosity. Greater porosity, in turn, leads to reduced compressive strength (Chen *et al.*, 2013). This finding aligns with the study of Ma *et al.* (2013), which reported that the use of OA decreases the compressive strength of cement. The persistence of these differences from the 7th to the 28th day indicates that the observed effects are long-lasting. These findings highlight the potential of OA-GO in improving mortar’s water resistance while cautioning against the use of OA alone, which may negatively impact durability.

Table 1. Mean Distribution of Contact Angle (CA) with One Way ANOVA Test

Day	Treatment Group	Mean ± 95%CI	F	P Value	Tukey Subset
Contact Angle (7 th Day)	M1	50.38 ± 14.59	31.38	0.0000	2
	M2	40.78 ± 26.88			2
	M3	98.50 ± 3.68			3
	M4	26.23 ± 3.22			1
Contact Angle (28 th Day)	M1	54.53 ± 7.19	55.66	0.0000	2
	M2	56.77 ± 23.67			2
	M3	115.82 ± 10.86			3
	M4	28.45 ± 5.10			1

To assess whether the measured contact angles changed between days 7 and 28 for each experimental group, a series of paired t-tests were conducted (Table 2). The results showed no significant changes in contact angles for M1, M2, and M4. However, in M3, the contact angle significantly increased from day 7 to day 28.

Further analysis was performed to determine whether the measured contact angles were hydrophobic (>90°) or hydrophilic (<90°). One-sample t-tests were conducted against the standard value of 90° (Table 3). The results indicated that only M3 (0.05% OA-GO) exhibited significantly hydrophobic behavior on both day 7 (t = 6.41, p = 0.0031) and day 28 (t = 6.61, p = 0.0027). This suggests that the combination of OA and GO effectively enhanced the water repellency of the mortar.

The observed increase in contact angle over time suggests that the hydrophobic effect of OA-GO strengthens as the mortar cures. In contrast, all

other groups remained hydrophilic, indicating they did not develop significant water-repellent properties. These findings support previous research showing that GO is highly hydrophilic due to presence of oxygen containing functional groups and does not substantially alter wettability (Rezaee *et al.*, 2015; Zhao *et al.*, 2013; Hegab and Zou, 2015; Junaidi *et al.*, 2018). However, OA appears to influence GO’s behavior, enhancing its hydrophobic effect. This highlights the potential of OA-GO as an effective hydrophobic admixture for cementitious materials.

Table 2. Independent Samples T-Test for Day 7 and 28 CA measurements

Treatment Group	Mean		<i>t</i> Value	<i>p</i> Value	Interpretation
	Day 7	Day 28			
M1	50.38	54.53	0.78	0.402	No significant change
M2	40.78	56.77	1.19	0.299	No significant change
M3	98.50	115.82	3.37	0.028	Significant increase
M4	26.23	28.45	1.37	0.243	No significant change

Table 3. Paired T-Test to compare measure CA against 90°

Treatment Group	Day	<i>n</i>	<i>t</i> Value	<i>p</i> Value	Interpretation	Remarks
M1	Day 7	5	7.54	0.0017	Significantly < 90°	Hydrophilic
	Day 28	5	13.70	0.0002	Significantly < 90°	Hydrophilic
M2	Day 7	5	5.09	0.0071	Significantly < 90°	Hydrophilic
	Day 28	5	3.90	0.0176	Significantly < 90°	Hydrophilic
M3	Day 7	5	6.41	0.0031	Significantly > 90°	Hydrophobic
	Day 28	5	6.61	0.0027	Significantly > 90°	Hydrophobic
M4	Day 7	5	46.44	0.0001	Significantly < 90°	Hydrophilic
	Day 28	5	33.53	0.0001	Significantly < 90°	Hydrophilic

3.4 Compressive strength test

Another set of specimens was subjected to a compressive strength test using the Universal Testing Machine (UTM). The mortars with 0.00% admixture (M1), 0.05% GO (M2), 0.05% OA-GO (M3), and 0.05% OA (M4) were tested for their compressive strength. The results were then analyzed, graphed, and compared to evaluate the impact of the different admixtures.

In Figure 6, it was observed that the reference mortar has the highest compressive strength among the mortars tested both for 7 and 28 days of curing. It was also noticed that the addition of GO in the mortar matrix did not

show a significant increase in compressive strength, although studies were reported to have positive progress in compressive strength (Gong *et al.*, 2015 and Kim *et al.*, 2018). This low compressive strength result may be due to the uneven distribution of the GO flakes in the mortar matrix during the hand mixing process or the minimal amount of GO used in fabricating the mortar.

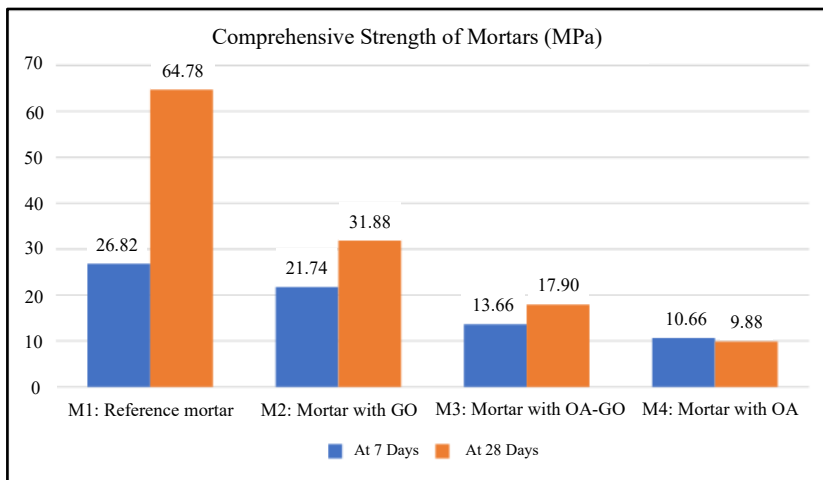


Figure 6. Compressive strength of mortars with 0.00% admixture (M1), mortar with 0.05% GO (M2), mortar with 0.05% OA-GO (M3), and mortar with 0.05% OA (M4).

On the other hand, the mortar with OA as an admixture was also tested. Results showed that its compressive strength is the lowest among the other mortars. The decrease in the compressive strength of the said mortar is due to the nature of OA, which is an unsaturated oil (Ma *et al.*, 2013; Albayrak *et al.*, 2005). An unsaturated oil contains double bonds that oxidize with the dissolved oxygen in the water during the curing period. This phenomenon also causes microscopic cracks in the cement (Ma *et al.*, 2013).

However, with the use of OA-GO, the compressive strength increases by a factor of 1.82 in 28 days of curing, which is almost twice that of the mortar with OA alone. Results showed that the capability of GO, which is to increase compressive strength, acts on the downside of the OA, which decreases the compressive strength of the mortar. It should also be observed that among the samples, the mortar with OA admixture shows a decrease in compressive strength after 28 days of the curing period. This is another problem that has been addressed with the introduction of OA-GO in the mortar matrix.

4. Conclusion and Recommendation

In summary, this study examined the effects of various admixtures on rendering mortars, including graphene oxide (GO), oleic acid-influenced graphene oxide (OA-GO), and oleic acid (OA). Statistical analyses revealed significant differences in contact angles among the tested mortars, with the OA-GO admixture displaying superior hydrophobic properties. Notably, the addition of GO to the OA admixture stabilized compressive strength and enhanced hydrophobicity, countering the negative effects observed with OA alone. These results suggest that the OA-GO admixture is effective in reducing water absorption while strengthening the mortar, making it a promising option for applications requiring resistance to water ingress. Overall, this study highlights the potential of the OA-GO admixture in enhancing water resistance and durability in rendering mortars or as external wall finishing.

5. Acknowledgement

The authors would like to acknowledge the Department of Physics, Central Mindanao University – for the laboratory space and equipment, and Mr. Angelito and Mrs. Lorna Panadero – for funding the experiment.

6. References

- Alam, S.N., Sharma, N., & Kumar, L. (2017). Synthesis of graphene oxide (GO) by modified Hummers method and its thermal reduction to obtain reduced graphene oxide (rGO). *Graphene*, 6(1), 1-10. <https://doi.org/10.4236/graphene.2017.61001>
- Albayrak, A.T., Yasar, M., Gurkaynak, M.A., & Gurgey, I. (2005). Investigation of the effects of fatty acids on the compressive strength of the concrete and the grindability of the cement. *Cement and Concrete Research*, 35(2), 400-404.
- American Society for Testing and Materials (ASTM) C192-15. (2015). Standard practice for making and curing concrete test specimens in the laboratory. West Conshohocken, PA: ASTM International.
- American Society for Testing and Materials (ASTM) C109/C109M-02. (2002). Standard test method for compressive strength of hydraulic cement mortars (Using 2-in. or [50-mm] cube specimens). West Conshohocken, PA: ASTM International.

Barnat-Hunek, D., & Smarzewski, P. (2015). Increased water repellence of ceramic buildings by hydrophobisation using a high concentration of organic solvents. *Energy and Buildings*, 103, 249–260. <https://doi.org/10.1016/j.enbuild.2015.06.048>

Bediako, M., Gawu, S.K.Y., & Adjaottor, A.A. (2012). Suitability of some Ghanaian mineral admixtures for masonry mortar formulation. *Construction and Building Materials*, 29, 667–671. <https://doi.org/10.1016/j.conbuildmat.2011.06.016>

Chen, J., Yao, B., Li, C., & Shi, G. (2013). An improved Hummers method for eco-friendly synthesis of graphene oxide. *Carbon*, 64, 225–229. <https://doi.org/10.1016/j.carbon.2013.07.055>

Chuah, S., Pan, Z., Sanjayan, J.G., Wang, C.M., & Duan, W.H. (2014). Nano-reinforced cement and concrete composites and new perspective from graphene oxide. *Construction and Building Materials*, 73, 113-124.

Di Mundo, R., Petrella, A., & Notarnicola, M. (2018). Surface and bulk hydrophobic cement composites by tyre rubber addition. *Construction and Building Materials*, 172, 176–184. <https://doi.org/10.1016/j.conbuildmat.2018.03.233>

Gong, K., Pan, Z., Habibnejad Korayem, A., Qiu, L., Li, D., Collins, F.G., Wang, C.M., & Duan, W. (2015). Reinforcing effects of graphene oxide on Portland cement paste. *Journal of Materials in Civil Engineering*, 27(2), 1-6.

Hegab, H.M., & Zou, L. (2015). Graphene oxide-assisted membranes: Fabrication and potential applications in desalination and water purification. *Journal of Membrane Science*, 484, 95–106.

Jeong, H.K., Jin, M.H., So, K.P., Lim, S.C., & Lee, Y.H. (2009). Tailoring the characteristics of graphite oxides by different oxidation times. *Journal of Physics D: Applied Physics*, 42(6), 065418. <https://doi.org/10.1088/0022-3727/42/6/065418>

Junaidi, N.F.D., Khalil, N.A., Jahari, A.F., Shaari, N.Z.K., Shahrudin, M.Z., Alias, N.H., & Othman, N.H. (2018). Effect of graphene oxide (GO) on the surface morphology & hydrophilicity of polyethersulfone (PES). *IOP Conference Series: Materials Science and Engineering*, 358, 012047. <https://doi.org/10.1088/1757-899X/358/1/012047>

Kim, B., Taylor, L., Troy, A., McArthur, M., & Ptaszynska, M. (2018). The effects of graphene oxide flakes on the mechanical properties of cement mortar. *Computers and Concrete*, 21(3), 261–267. <https://doi.org/10.12989/CAC.2018.21.3.261>

Krishnamoorthy, K., Veerapandian, M., Yun, K., & Kim, S.-J. (2013). The chemical and structural analysis of graphene oxide with different degrees of oxidation. *Carbon*, 53, 38-49. <https://doi.org/10.1016/j.carbon.2012.10.013>

Lanzón, M., & García-Ruiz, P.A. (2009). Evaluation of capillary water absorption in rendering mortars made with powdered waterproofing additives. *Construction and Building Materials*, 23(10), 3287-3291.

Luan, Y., Furuta, H., Asamoto, S., & Yoneda, T. (2016). A study of properties of mortar mixed with hydrophobic agents: Water absorption, strength and drying

shrinkage. Proceedings of 4th International Symposium on Advances in Civil and Environmental Engineering Practices for Sustainable Development, 1, 213-220.

Ma, B., Wang, J., Li, X., He, C., & Yang, H.M. (2013). The influence of oleic acid on the hydration and mechanical properties of Portland cement. *Journal of Wuhan University of Technology-Materials Science Edition*, 28, 1177-1180.

Muzenski, S.W., Flores-Vivian, I., & Sobolev, K. (2014). The development of hydrophobic and superhydrophobic cementitious composites. Proceedings of the 4th International Conference on the Durability of Concrete Structures, ICDCS 2014. <https://doi.org/10.5703/1288284315484>

Naval Civil Engineering Laboratory. (2009). Technical Report. Naval Civil Engineering Laboratory (Port Hueneme, Calif.), 190-198.

Rezaee, R., Nasser, S., & Mahvi, A.H. (2015). Fabrication and characterization of a polysulfone-graphene oxide nanocomposite membrane for arsenate rejection from water. *Journal of Environmental Health Science and Engineering*, 13(61). <https://doi.org/10.1186/s40201-015-0217-8>

Romani, A. (2015). Graphene oxide as a cement reinforcement additive: Preliminary study (Master's thesis, Politecnico di Milano).

Sharma, N., & Sharma, P. (2021). Effect of hydrophobic agent in cement and concrete: A review. *IOP Conference Series: Materials Science and Engineering*, 1116, 012175. <https://doi.org/10.1088/1757-899X/1116/1/012175>

Shen, J., Shi, M., Yan, B., Ma, H., Li, N., & Ye, M. (2011). One-pot hydrothermal synthesis of Ag-reduced graphene oxide composite with ionic liquid. *Journal of Materials Chemistry*, 21(21), 7795–7801. <https://doi.org/10.1039/C1JM10671F>

Somanathan, T., Prasad, K., Ostrikov, K., Saravanan, A., & Mohana Krishna, V. (2015). Graphene oxide synthesis from agro waste. *Nanomaterials*, 5(2), 826-834.

Song, J., Wang, X., & Chang, C.T. (2014). Preparation and characterization of graphene oxide. *Journal of Nanomaterials*, 2014, 276143. <https://doi.org/10.1155/2014/276143>

Zhang, Y., & Pan, C. (2011). TiO₂/graphene composite from thermal reaction of graphene oxide and its photocatalytic activity in visible light. *Journal of Materials Science*, 46(8), 2622–2626. <https://doi.org/10.1007/s10853-010-5116-x>

Zhao, C., Xu, X., Chen, J., & Yang, F. (2013). Effect of graphene oxide concentration on the morphologies and antifouling properties of PVDF ultrafiltration membranes. *Journal of Environmental Chemical Engineering*, 1, 349–354.

Zhou, L., Wang, W., Tang, J., Zhou, J.-H., Jiang, H.-J., & Shen, J. (2011). Graphene oxide noncovalent photosensitizer and its anticancer activity *in vitro*. *Chemistry – A European Journal*, 17(5), 1209–1215. <https://doi.org/10.1002/chem.201003078>